International Journal of Applied Pharmaceutics

ISSN- 0975-7058 Vol 15, Issue 5, 2023

Original Article

IN SILICO MOLECULAR SCREENING AND DOCKING APPROACHES ON ANTINEOPLASTIC AGENT-IRINOTECAN TOWARDS THE MARKER PROTEINS OF COLON CANCER

MAHALEKSHMI V.[1,3], BALAKRISHNAN N.[3], AJAY KUMAR T. V.[4], PARTHASARATHY V.[1,2,5*]

[1]Department of Pharmacy, Annamalai University, Annamalai Nagar-608002, Tamilnadu, India. [2]Immunology Laboratory, Department of Pharmacy, Annamalai University, Annamalai Nagar-608002, Tamilnadu, India. [3]S. A. Raja Pharmacy College, Vadakangulam, Tirunelveli, Tamilnadu-627116, India. [4]Azidus Laboratories Ltd., Rathinamangalam, Vandalur, Chennai-600048, Tamilnadu, India. [5]Centre for Cell Biology and Drug Discovery, Faculty of Engineering, Annamalai University, India

[*]Corresponding author: Parthasarathy V.; [*]Email: vapartha@yahoo.com

Received: 05 Jun 2023, Revised and Accepted: 01 Aug 2023

ABSTRACT

Objective: The present investigation explores the binding affinities of Irinotecan, which is a topoisomerase I inhibitor, against the targets such as AKT1, TNKS-2, MMP, EGFR, TNKS-1, and BRAF, which are the protein that was overexpressed by colorectal carcinogenesis.

Methods: In this study, the drug structure was drawn by chemdraw software and explored for its anti-cancer potential by Schrodinger software against selected targeted proteins such as epidermal growth factor receptor (EGFR), matrix metalloproteinase (MMPs), serine/threonine protein kinase Ba (AKT1), BRAF, tankyrases 1 (TNKS-1, and tankyrases 2 (TNKS-2).

Results: From the results of docking analysis, the targets with the maximum binding affinity towards the preselected drug Irinotecan were further subjected to ADME prediction by the QikProp module of Schrodinger Maestro version 2018.4. Molecular docking analysis revealed that surface protein targets AKT1, TNKS-2, MMP, and EGFR have the highest binding affinity towards the selected topoisomerase I inhibitor Irinotecan when compared to TNKS-1 and BRAF targets. The higher docking score of Irinotecan with extracellular colorectal cancer target proteins was discovered in this investigation.

Conclusion: Cancer is one of the most prevalent, lethal and risky malignant pathologies with an elevated prevalence and mortality rate worldwide. The current work will be more beneficial for rationalising the effective anticancer treatment according to the intensities of expression of the colon cancer target protein and for creating an optimum targeted drug delivery system of an anticancer agent to treat colon cancer.

Keywords: Colorectal cancer, Irinotecan hydrochloride, Marker proteins, Molecular Docking, Lipinski's rule

DOI: https://dx.doi.org/10.22159/ijap.2023v15i5.48523. Journal homepage: https://innovareacademics.in/journals/index.php/ijap

INTRODUCTION

Cancer is a physiological condition that develops as a consequence of the body's cells proliferating abnormally. Globally, cancer is widespread in mostly six organs: lung, breast, colorectal, prostate, stomach and cervical [1, 2]. Colorectal cancer (CRC), ranks among the most extensive and third most chief causes of death, driven on by some genetic changes in the colorectal mucosal lining and has emerged as a serious global health problem. In 2020, it is anticipated that there would be 1.93 million new cases of CRC diagnosed and 0.94 million deaths globally [3, 4]. Despite variations in mortality rates, population growth and ageing are expected to cause the number of deaths from colon and rectal cancer to increase by 60.0% and 71.5%, respectively, in all countries through 2035. With an expected 2.4 lakh diagnoses by 2035, increased access to early detection services and specialised care is most likely responsible for the decreased mortality rates for colon and rectal cancer [5, 6]. Both changeable and immutable components are risk factors for Colon cancer (CC). Age and genetic predisposition are risk factors that cannot be modified; hence it is highly recommended to have people over 50 and/or with a family history of polyps and CRC examined [7]. Red and processed meat intake, alcohol use, and diets that are heavy in fat and low in fibre have all been related to an amplified risk of CC or CRC [8, 9]. Smoking, being overweight, and some other risk factors contribute to cancer development. Apoptosis usually stops damaged cells from becoming out of balance under normal physiological circumstances is avoided and control apoptosis [10]. FDA-approved drugs such as capecitabine, 5-fluorouracil, irinotecan, oxaliplatin, and trifluridine/tipiracil are commonly used anticancer drugs for chemotherapy [11-13]. Oxaliplatin (OX), irinotecan (IRI), and capecitabine are examples of medications used in multiple-agent chemotherapy. Various chemotherapy regimens, either alone or in combination, are used as current treatments for CRC. Examples include FOLFOXIRI (5-FU/oxaliplatin/irinotecan), FOLFIRI (5-FU/leucovorin/oxaliplatin), and FOLFOX (5-FU/leucovorin/oxaliplatin). High-grade toxicity includes neurological diseases, gastrointestinal side effects, myelosuppression, neutropenia, anaemia, etc causes frequently necessitates dose restrictions or the termination of anticancer therapy [14-16]. The important drug targets for colon cancer include Epidermal growth factor receptor (EGFR) [17], Matrix metalloproteinase (MMP) [18, 19], Serine/threonine protein kinase Ba (AKT1) [20], BRAF [21, 22], tankyrases 1 and 2 (TNKS-1 and TNKS-2) [23, 24], Mitogen-activated protein kinase 3 (MAPK3) [25, 26], Human tyrosine-protein kinase (C-SRC) [27, 28], Tumour suppressor p53 (TP53) [29-31], Glyceralde-3-phosphate dehydrogenase (GAPDH) [32, 33], poly (ADP-ribosyl) polymerase 1 (PARP) [34, 35], inducible nitric oxide synthase (iNOS) [36-38], Checkpoint kinase 1 (Chk1) [39-41], and so on.

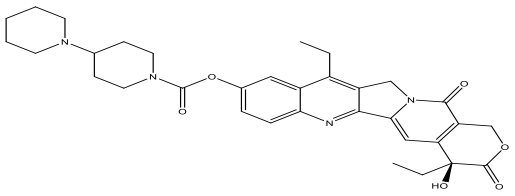

Fig. 1: Structure of Irinotecan, (4S)-4,11-diethyl-4-hydroxy-9-([4-piperidino-piperidino] carbonyloxy)1H-pyrano(3′,4′:6,7) indolizino (1,2-b) quinol-3,14, (4H,12H)-dione hydrochloride or 7-ethyl-10-(4-[1-piperidino]1-piperidino) carbonyloxy camptothecin

Irinotecan (IRT) is an alkaloid extract from the plant *Camptotheca acuminata* that is water-soluble and semi-synthetic in nature.

Chemically, irinotecan is irinotecan hydrochloride trihydrate (4S)-4,11-diethyl-4-hydroxy-9-([4-piperidino-piperidino] carbonyloxy). 1H-pyrano (3′, 4′: 6, 7) indolizino (1,2-b) quinol-3,14 (4H, 12H)-dione hydrochloride or 7-ethyl-10-(4-[1-piperidino]-1-piperidino) carbonyloxy camptothecin. For the treatment of colorectal cancer which is resistant to 5-fluorouracil (5-FU), it has received FDA approval as a first-line chemotherapeutic medication [42-44]. IRT is transformed in living cells into the active metabolite 7-ethyl-10-hydroxycamptothecine (SN-38), which attaches to the topoisomerase I-DNA complex, and prevents DNA strand breaks from being relegated, and causes cytotoxicity [43, 45, 46].

Molecular docking analysis is essential for discovering new drugs as well as determining how drugs interact with molecules and receptors. The primary goal of the current investigation was to use *in silico* docking analysis against the chosen targets to determine the degree of specificity of the chemical component irinotecan for its potential anti-cancer effect on colon cancer and to overcome the side effects of the drug by releasing IRT directly into the cancer cells. The colon cancer-specific marker proteins chosen for the present study are, among others, EGFR, MMP, AKT1, BRAF, TNKS-1, and TNKS-2. Schrödinger software was employed to carry out the investigation. The protein data bank (PDB) was used to mine these proteins. In addition to this, the Lipinski rule was used to predict the drug similarity and the ADME (absorption, distribution, metabolism, and excretion) characteristics of Irinotecan. The transmembrane glycoprotein known as the epidermal growth factor (EGF) receptor is a member of the tyrosine kinase receptor family. The binding of EGF to its cognate ligands might result in autophosphorylation and subsequent signal transduction pathways (cellular proliferation, differentiation, and survival) [47, 48]. Matrix metalloproteinases (MMPs) are proteolytic enzymes that are zinc-dependent metalloproteinases that have the potential to break down the proteins in the extracellular matrix (ECM) [24, 49-52]. AKT, or Protein Kinase B, is a protein kinase (PKB), a serine/threonine kinase that stops apoptosis, governs glycogen metabolism, and encourages the growth of cancer. AKT that has been phosphorylated and overexpressed is a therapeutic target for the management of malignant tumours [53]. AKT activation regulates apoptosis as well as the cell cycle, cell motility, and angiogenesis, which promote cell transformation and cancer [54]. The B-Raf proto-oncogene, serine/threonine kinase gene (BRAF), is a critical molecular genomic marker utilised in CRC diagnosis, prognosis, and therapy modalities [55]. The BRAF gene participates in the MAPK/ERK signalling pathway, which is crucial for the development of cancer and other diseases (RASopathies). This route influences crucial cell processes such as proliferation, senescence, apoptosis, differentiation, and growth [56, 57]. Tankyrases are members of the two-membered family of proteins known as poly (ADP)-ribose polymerases (PARPs): tankyrase 1 (TNKS-1) and tankyrase 2 (TNKS-2) [23]. Tankyrase exerts positive control on the Wnt/b-catenin signalling pathway, which is amplified in the early stages of colorectal cancer development [58].

MATERIALS AND METHODS

Preparation of protein

Three-dimensional (3D) crystal structures of the proteins, namely, epidermal growth factor receptor (EGFR) (PDB code: 1M17), matrix metalloproteinase (MMPs) (PDB code: 2DDY), serine/threonine protein kinase Ba (AKT1) (PDB code: 3O96), BRAF (PDB code: 4MNE), Tankyrases 1 (TNKS-1) (PDB code: 5ECE), and Tankyrases 2 (TNKS-2) (PDB code: 6KRO) were recognised and imported from the Protein Data Bank (PDB) (http://www.rcsb.org/pdb/-home/home.do). The resolutions of the target proteins are 2.60 Å (1M17), 2.31 Å (2DDY), 2.70 Å (Akt 1), 2.85 Å (BRAF), and 2.20 Å (Tankyrases 1) and were considered good for further analysis. "Protein preparation wizard" was used to import the proteins' 3D structures. Using the required modelling calculations of Schrodinger software, the protein was created in this manner. A protein structure with heavy atoms, metal ions, missing hydrogen atoms, water molecules, co-crystallised ligands, and incomplete and terminal amide groups may be found and extracted using the protein data bank. The wizard fixed the bond ordering, made formal adjustments, added the missing protons, treated the metals, and got rid of the water that extended past the heteroatom's 5th position. Using Epik, the potential ionisation states for the protein's ligand were produced, and the most stable state was chosen [59]. Using the force field OPLS-2005 and a restricted root mean square deviation (RMSD) tolerance of 0.3, the protein was then minimised under controlled conditions [60].

Receptor grid generation

The "receptor grid creation" feature was used to create the grid over the ligands associated with an active site while keeping the ligands present in all proteins. The protein's active site is indicated by the centroid (cubical) shape that forms over the ligand [61, 62].

Ligand preparation

Irinotecan chemical structure and formula (C33H38N4O6) were created using "Chemdraw" and then saved in SDF format (fig. 1). The ligand was then loaded into Schrodinger 2018's "LigPrep" module software. The molecule's 2D structure was changed into a low-energy 3D structure [63]. These were added to by the creation of several structures with various ionisation states: tautomers, stereo-isomers, and ring conformations. The ligand was also tuned for its shape and energy minimization. Ionisation and tautomeric states were produced in a pH range of 6.8 to 7.2 using the "EPIK" module. The optimal potentials for liquid simulations-2005 (OPLS-2005) force field was used to decrease the compounds, yielding a root mean square deviation (RMSD) value of 1.8 [64].

Molecular docking

The formerly chosen receptor grid and ligand were used throughout the docking procedure, which was carried out using the Schrodinger "Glide" module [65, 66]. Using the Glide "Ligand docking" tool, the favourable contacts between the ligand molecules were rated. The extra precision (XP) form and force field of OPLS-2005 were used to perform the docking calculations. The docking postures were changed using a series of hierarchical filters, and the flexible docking mode was used to assess how well the ligand connected to the receptor. The strategy minimises steric collisions while emphasising advantageous metal ligation, hydrogen bonds, and hydrophobic interactions. The method's last phase involves rating the reduced postures using the Glide "Scoring function" and force field OPLS-2005 minimization [67].

"Lipinski's rule of five (Ro5)" and the analysis of pharmacokinetics (ADME) properties

To prevent the failure of a molecule at the end of the drug development process, *in silico* analysis is a crucial method for early preclinical evaluation of a novel chemical entity. Using this method, the processes for expanding medicinal molecules are rationalised, and time and resources are greatly saved. Almost 40% of drug candidates fail owing to inadequate pharmacokinetic properties such as absorption, distribution, metabolism, and excretion (ADME) characteristics. In order to accurately predict the ADME properties of a freshly created molecule and to screen challenging drug candidates that shouldn't be explored further, high-throughput screening (HTS) techniques are used. Amazingly, using this technique, the failed chemical is changed to enhance its beneficial characteristics [68].

The preferred filter, Lipinski's Rule of Five (Ro5), is more effective in predicting a molecule's bioavailability. According to the five requirements in 2004 (Lipinski), the molecular mass should be less than 500 daltons, there should be no more than five hydrogen bond donors and no more than ten hydrogen bond acceptors, and the "log P" octonal/water partition coefficient should be less than five. The Schrodinger 2018.1 "QikProp" tool was used to forecast Lipinski's Rule of Five (Ro5), and pharmacokinetic characteristics such as absorption, distribution, metabolism, and excretion (ADME) (Schrodinger, 2018) [69-71].

RESULTS AND DISCUSSION

Using the sophisticated molecular docking programme "Schrodinger Maestro version 11," several target proteins in colon cancer and the ligand "Irinotecan" were studied on the active sites. The "LigPrep" tool from Schrodinger software was used to optimise the ligand

irinotecan, which was then used for docking experiments. The colon cancer proteins EGFR, MMP, AKT1, BRAF, TNKS-1, and TNKS-2 were made using the protein preparation wizard programme of Schrodinger. Schrodinger's receptor grid creation method was used to build the cube-shaped grid/active site area. The selected and set-up Grid region or active site was designed to bind or interact with the target drug, "Irinotecan." The research rated the binding affinity of irinotecan for each of its target proteins. Binding orientations of Irinotecan with the crystal structure of EGFR, MMP, AKT1, BRAF, TNKS-1, and TNKS-2 was given in fig. 1-7.

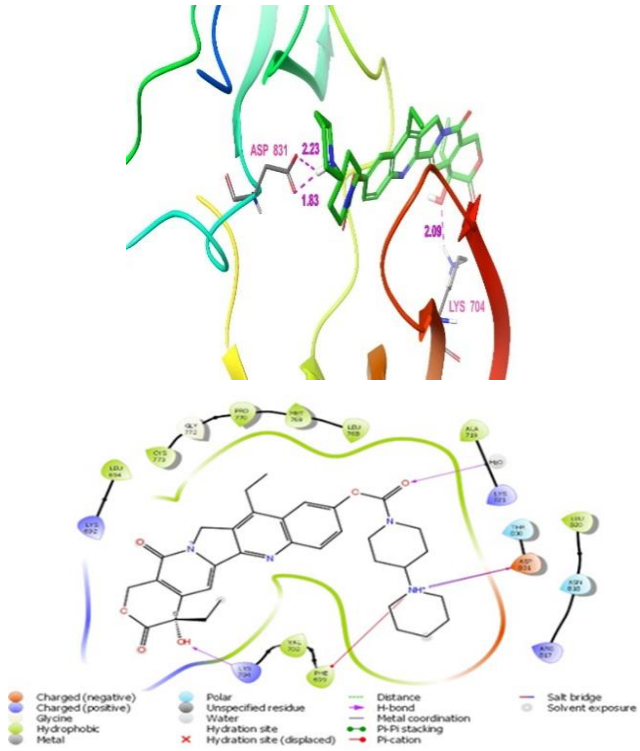

Fig. 2: Binding orientations of Irinotecan with the crystal structure of Epidermal growth factor receptor (EGFR) and its hydrogen-bond interactions with amino acids

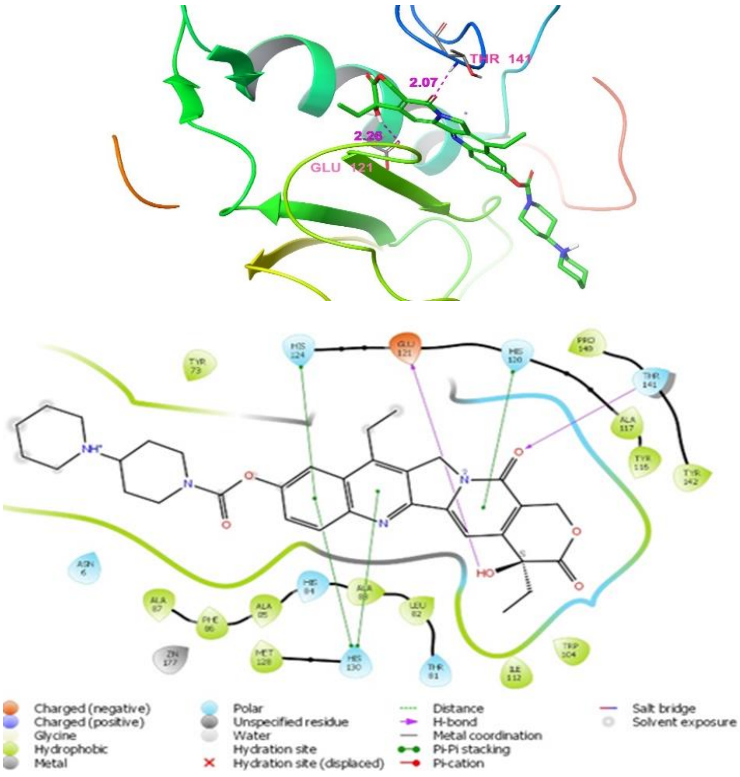

Fig. 3: Binding orientations of Irinotecan with the crystal structure of matrix metalloproteinase (MMPs) and its hydrogen-bond interactions with amino acids

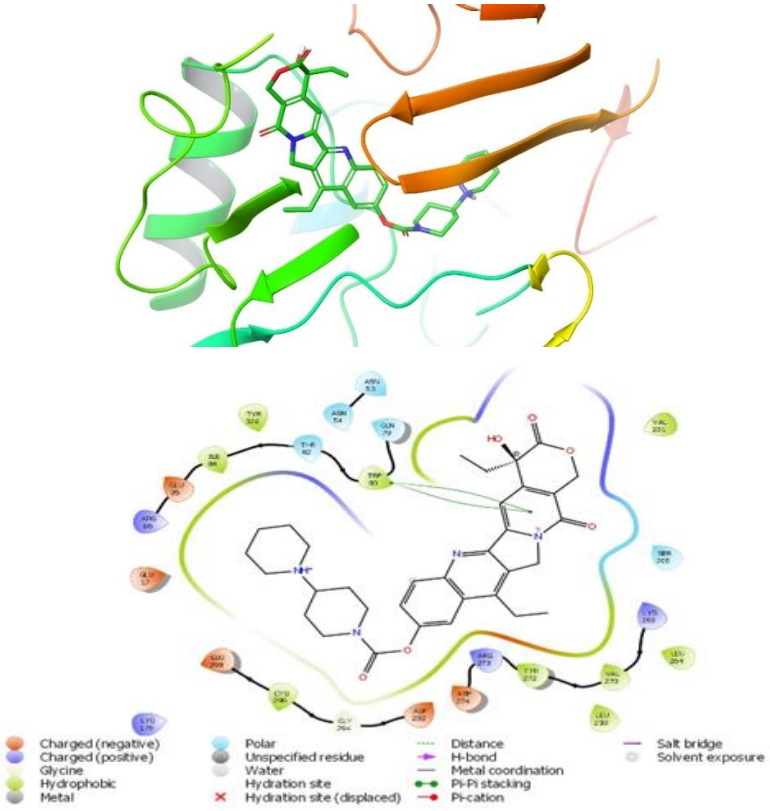

Fig. 4: Binding orientations of Irinotecan with the crystal structure of serine/threonine protein kinase Ba (AKT1) and its hydrogen-bond interactions with amino acids

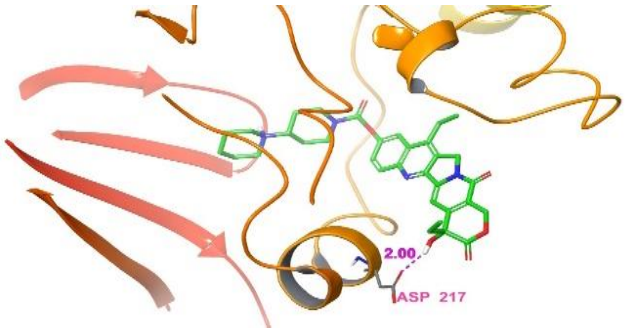

Fig. 5: Binding orientations of Irinotecan with the crystal structure BRAF

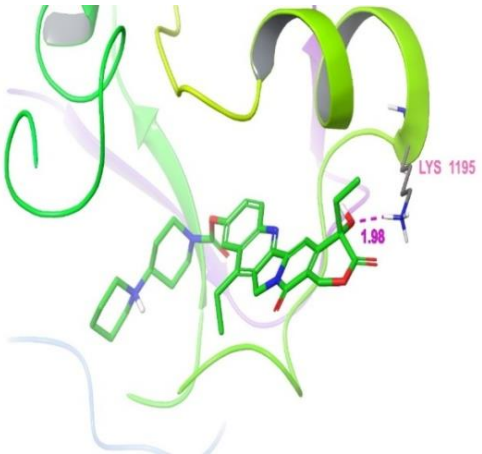

Fig. 6: Binding orientations of Irinotecan with the crystal structure of Tankyrases 1 (TNKS-1)

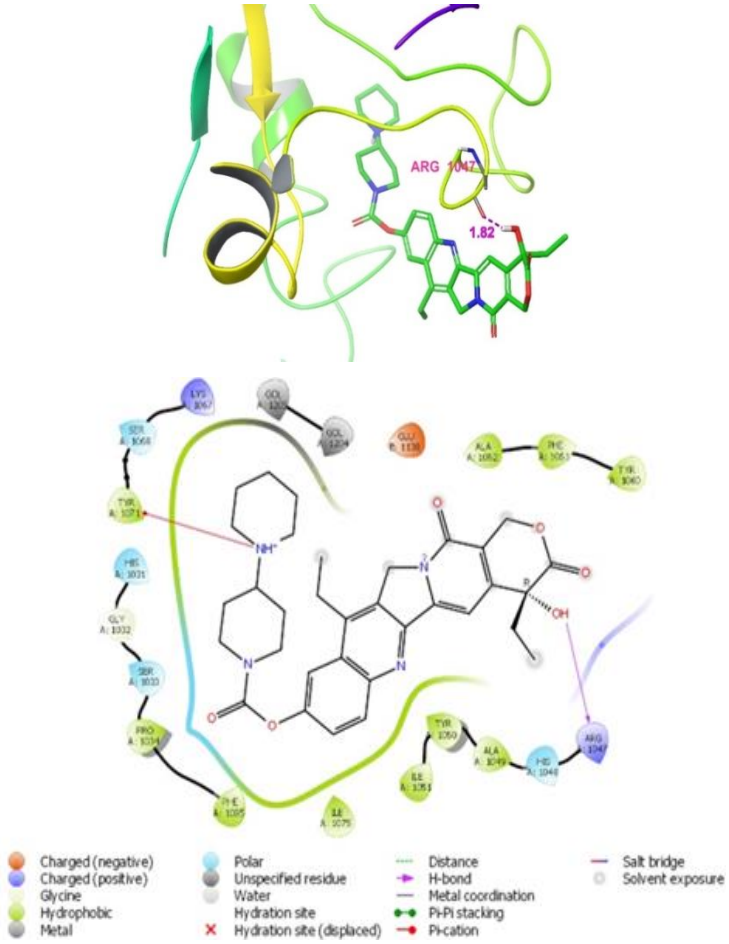

Fig. 7: Binding orientations of Irinotecan with the crystal structure of Tankyrases 2 (TNKS-2) and its hydrogen-bond interactions with amino acids

Using schrodinger's GLIDE programme, molecular docking was done on all target proteins, including EGFR, MMP, AKT1, BRAF, TNKS-1, and TNKS-2. The predicted values of docking score, Glide evdw (Van Der Waals energy), ecoul (Coulomb energy), Glide energy, and the interacting residues (Hydrogen bond/-bond) were all carefully examined to ascertain the extent of interaction between the target proteins and Irinotecan. The study's findings indicated that the ligand "Irinotecan" docked well and made powerful binding with the active sites of all the proteins. The results for EGFR, MMP, AKT1, BRAF, TNKS-1, and TNKS-2 were labelled by the protein codes 1M17, 2DDY, 3O96, 4MNE, 5ECE, and 6KRO, respectively (table 1). The protein targets such as EGFR, MMP, AKT1, BRAF, TNKS-1, and TNKS-2 found in this study is overexpressed is a therapeutic target for the management of malignant tumours (47-58). IRT attaches to the topoisomerase I-DNA complex and prevents DNA strand breaks from being relegated and causes cytotoxicity [43, 45, 46]. The current investigation found that irinotecan interacted well with all of the targeted proteins, with the order of binding being AKT1>TNKS-2>MMP>EGFR>TNKS-1>BRAF. The docking scores of the proteins are as follows: -8.70,-7.62,-6.52,-5.68,-4.34, and-3.54. A high binding affinity option is the ligand with the lowest binding energy. In this investigation, AKT1 and TNKS-2 had greater binding affinities to Irinotecan than MMP, EGFR, TNKS-1, and BRAF proteins. AKT1, TNKS-2, MMP, EGFR, TNKS-1, and BRAF had Glide evdv values of-60.46,-36.72,-47.15,-42.01,-42.47, and-34.44, respectively (table 1).

Glide energy values f were-4.05,-3.18,-8.48,-9.05,-6.41, and-4.45. Following that, the glide energies of proteins such as AKT1, TNKS-2, MMP, EGFR, TNKS-1, and BRAF were calculated, and the results are-38.87,-39.90,-55.63,-51.06, and-48.88, respectively. The target proteins amino acids in particular, displayed excellent interaction with Irinotecan via hydrogen bonding, pi-pi bonding, and polar interactions. Table 1 shows the hydrogen bonds and pi-pi interactions formed by target protein amino acids and Irinotecan. Each target protein's docking scores with "Irinotecan" were compared. Interestingly, the drug "Irinotecan" showed excellent binding interactions and affinities with all six proteins that are specific for colon cancer, with the following order of binding interactions: AKT1>TNKS-2>MMP>EGFR>TNKS-1>BRAF. By considering the ligand and certain target areas as flexible conformations, this approach was able to determine the binding free energy between each target and ligand. IRT demonstrated the least amount of binding energy to AKT1 of all the examined proteins. Additionally, compared to other targets, AKT1 is one of the targets in cancer research that has received the most attention. Several anticancer candidates that target AKT1, such as capivasertib (AZD5363), ipatasertib (RG7440), and MK-2206, are currently undergoing clinical trials [72]. MK-2206, one of these contenders, has demonstrated good outcomes in the treatment of people with colorectal cancer [73].

Evaluation of the docking programme

The docking procedure's accuracy was demonstrated by the scoring function's analysis of the binding conformations of the ligand and target proteins based on their lowest energy positions. The experimental binding as measured by X-ray crystallography and the Glide/docking score are equivalent. The investigation's conclusions were calculated using hydrogen bonding interactions and the root mean square deviation (RMSD) between the anticipated and actual X-ray crystallographic conformations. By removing the co-crystallised ligand from its active site, "Irinotecan" was docked with its binding site to demonstrate the extreme precision (XP) docking mode [73]. The docking scores of each target protein with "Irinotecan" were compared. Surprisingly, "Irinotecan" showed

substantial binding contacts with each of the six proteins believed to be responsible for colon cancer, and their interactions were conducted in the order shown below: AKT1>TNKS-2>MMP>EGFR>TNKS-1>BRAF.

Table 1: Irinotecan's molecular docking score, glide evdw (Van der Waals energy), ecoul (Coulomb energy), interacting residues, kind of interaction, and docking score were determined using schrodinger's glide software (version 2018-1). Where the letters HB stand for hydrogen bonds and Pi-Pi for-bonds

Compound	Protein	Docking score	Glide evdw	Glide ecoul	Glide energy	Interacting residues/type (HB/Pi-Pi)
Irinotecan	1M17	-05.68	-42.01	-09.05	-51.06	LYS704, ASP831 and HOH
	2DDY	-06.52	-47.15	-08.48	-55.63	HIS120, GLU121 and THR141/HIS124 and HIS130
	3O96	-08.70	-60.46	-04.05	-64.51	TRP80
	4MNE	-03.54	-34.44	-4.45	-38.87	ASN78, LYS97, SER150, SER194, LYS192, LEU197 and HOH
	5ECE	-04.34	-42.47	-6.41	-48.88	LYS1195, TYR1203/PHE1188
	6KRO	-07.62	-36.72	-3.18	-39.90	ARG1047 and TYR1071

Lipinski rule and pharmacokinetic (ADME) parameters

The ADME characteristics of the test drug "Irinotecan" were further evaluated using the QikProp module of the Schrodinger software. Examples of Lipinski characteristics include molecular weight, hydrogen bond donor (HBD), hydrogen bond acceptor (HBA), partition coefficient (QPlogP (O/W), and the rule of five. The expected values for each of these parameters were, accordingly, 586.68 (500), 1 (5), 12.75 (10), and 3.41 (5), and the rule of five is one (0) (table 2). Except for a tiny change with HBA, the estimated Lipinski values were below the limit stated in parentheses.

Aqueous solubility (QPlogS), predicted IC50 for HERG K+channel blockage (QPlogHERG), blood and brain partition coefficient (QPlogBB), qualitative human oral absorption (PHOA), and gastrointestinal system barrier and cell permeability in nm/s (QPPCaco) were all calculated. The following values are equivalent: -6.5 (-6.50 to 0.50),-7.01 (-05),-1.32 (-03 to 1.20), 65 (>80 high, 25 poor), and 68 (>500 high, 25 poor) (table 3). The levels of irinotecan were within the permitted range and did not exceed the limit according to the pharmacokinetic characteristics of the drug. The complete experiment's findings demonstrated that irinotecan complied with all ADME and Lipinski's rule requirements and exhibited a consistent interaction with the target protein.

Table 2: The values that the lipinski rule-based QikProp module of schrodinger predicted for irinotecan. Molecular weight, abbreviated as M. W., the HB-Hydrogen bond, and the expected octanol/water partition coefficient logP together with the HB-Hydrogen bond and QPLogP (O/W)

Factors of lipinski rule of 5					
Name of the compound	**M. W. (<500)**	**HB-Donor (<05)**	**HB-Acceptor (<10)**	**QPlogP (O/W) (<05)**	**Rule of 5 (00)**
Irinotecan hydrochloride	586.68	01	12.75	03.41	01

Table 3: Irinotecan's ADME values were predicted using a schrodinger QikProp module. Where QPlogS stands for aqueous solubility, QpHERG for expected IC50 for blocking HERG K+channels, QPlogBB for predicted blood and brain partition coefficient, PHOA for predicted oral absorption, and QPPCaco for predicted gut-blood barrier and cell permeability in nm/s, respectively

Pharmacokinetic (ADME) properties					
Compound	**QPlogS (-06.50 to 0.50)**	**QpHERG (<-05)**	**QPlogBB (-03 to 01.20)**	**PHOA (>80 high,<25 poor)**	**QPPCaco (>500 high,<25 poor)**
Irinotecan	-06.5	-07.01	-01.32	65	68

CONCLUSION

The current work used Schrodinger Maestro to examine the molecular interactions and pharmacokinetics of Irinotecan with the chosen proteins AKT1, TNKS-2, MMP, EGFR, TNKS-1, and BRAF. Both binding affinity and ADME features were examined using Schrodinger's GLIDE and QikProp programmes. The results of the investigation showed that the individual proteins had strong hydrogen bonds, polar bonds, and pi-pi bonds with each other for binding. Interestingly, the expected scores for Irinotecan using Lipinski's rule and pharmacokinetic (ADME) characteristics were within satisfactory limits. As a result, the drug Irinotecan efficiently and at a low energy level inhibits the target colon cancer proteins AKT1, TNKS-2, MMP, EGFR, TNKS-1, and BRAF. Irinotecan's interactions with the six proteins were more energetic in the following order: AKT1>TNKS-2>MMP>EGFR>TNKS-1>BRAF. Additionally, compared to MMP, EGFR, TNKS-1, and BRAF proteins, the proteins AKT1 and TNKS-2 had higher binding affinities to irinotecan. In this current study, we identified the higher docking score of irinotecan with extracellular colorectal cancer target proteins. This study is recommended for the continuous effort of researchers towards the selected extracellular colorectal cancer target proteins that are most suitable with irinotecan hydrochloride as a candidate for pharmaceutical formulation.

DISCLAIMER

The products selected in this study are those that are often and predominately used in our nation and field of study. Because we don't aim to use these items as a venue for any lawsuit but rather for the development of knowledge, The authors and the product's makers have no financial ties to one another. Additionally, the study was not paid for by the production business; rather, the writers paid for it themselves.

LIST OF ABBREVIATIONS

AKT1-Serine/threonine protein kinase, TNKS–tankyrases, MMP-Matrix metalloproteinase, EGFR-Epidermal growth factor receptor, and BRAF, Irinotecan-IRT, Checkpoint kinase 1-Chk1, inducible nitric oxide synthase–iNOS, GAPDH-Glyceralde-3-phosphate dehydrogenase, MAPK3-Mitogen-activated protein kinase 3, PARP-poly (ADP-ribosyl) polymerase 1, TP53-Tumour suppressor p53, IRT-Irinotecan, ADME-Absorption, distribution, metabolism, excretion, HBD-hydrogen bond donor, HBA-hydrogen bond acceptor, RMSD-root mean square deviation.

FUNDING

This research did not receive a specific grant from any funding agencies.

CONFLICT OF INTERESTS

The authors declare no conflict of interest.

AUTHORS CONTRIBUTIONS

All the authors have contributed equally.

REFERENCES

1. Ferlay J, Soerjomataram I, Dikshit R, Eser S, Mathers C, Rebelo M. Cancer incidence and mortality worldwide: sources, methods and major patterns in Globocan 2012. Int J Cancer. 2015 Mar 1;136(5):E359-86. doi: 10.1002/ijc.29210, PMID 25220842.
2. Siegel R, DeSantis C, Jemal A. Colorectal cancer statistics, 2014. CA Cancer J Clin. 2014;64(2):104-17. doi: 10.3322/caac.21220, PMID 24639052.
3. International WCRF. Available online: https://www.wcrf.org/int/cancer-facts-figures.
4. Xi Y, Xu P. Global colorectal cancer burden in 2020 and projections to 2040. Transl Oncol. 2021 Oct 1;14(10):101174. doi: 10.1016/j.tranon.2021.101174, PMID 34243011.
5. Araghi M, Soerjomataram I, Jenkins M, Brierley J, Morris E, Bray F. Global trends in colorectal cancer mortality: projections to the year 2035. Int J Cancer. 2019 Jun 15;144(12):2992-3000. doi: 10.1002/ijc.32055, PMID 30536395.
6. Araghi M, Arnold M, Rutherford MJ, Guren MG, Cabasag CJ, Bardot A. Colon and rectal cancer survival in seven high-income countries 2010-2014: variation by age and stage at diagnosis (the ICBP SURVMARK-2 project). Gut. 2021 Jan 1;70(1):114-26. doi: 10.1136/gutjnl-2020-320625, PMID 32482683.
7. Simon K. Colorectal cancer development and advances in screening. Clin Interv Aging. 2016 Jul 19;11:967-76. doi: 10.2147/CIA.S109285, PMID 27486317.
8. Pan P, Yu J, Wang LS. Colon cancer: what we eat. Surg Oncol Clin N Am. 2018 Apr 1;27(2):243-67. doi: 10.1016/j.soc.2017.11.002, PMID 29496088.
9. Testino G, Leone S, Sumberaz A, Borro P. Alcohol and cancer. Alcohol Clin Exp Res. 2015;39(11):2261. doi: 10.1111/acer.12858, PMID 26332802.
10. Nelson AR, Fingleton B, Rothenberg ML, Matrisian LM. Matrix metalloproteinases: biologic activity and clinical implications. J Clin Oncol. 2000;18(5):1135. doi: 10.1200/JCO.2000.18.5.1135, PMID 10694567.
11. Geng F, Wang Z, Yin H, Yu J, Cao B. Molecular targeted drugs and treatment of colorectal cancer: recent progress and future perspectives. Cancer Biother Radiopharm. 2017 Jun 1;32(5):149-60. doi: 10.1089/cbr.2017.2210, PMID 28622036.
12. Ortega J, Vigil CE, Chodkiewicz C. Current progress in targeted therapy for colorectal cancer. Cancer Control. 2010 Jan;17(1):7-15. doi: 10.1177/107327481001700102, PMID 20010514.
13. Van Cutsem E, Cervantes A, Nordlinger B, Arnold D, ESMO Guidelines Working Group. Metastatic colorectal cancer: ESMO clinical practice guidelines for diagnosis, treatment and follow-up. Ann Oncol. 2014;25Suppl 3:iii1-9. doi: 10.1093/annonc/mdu260, PMID 25190710.
14. Alam W, Bouferraa Y, Haibe Y, Mukherji D, Shamseddine A. Management of colorectal cancer in the era of COVID-19: challenges and suggestions. Sci Prog. 2021 Apr;104(2):368504211010626. doi: 10.1177/00368504211010626, PMID 33878982.
15. Pointet AL, Taieb J. Cancro del colon. EMC-AKOS-Trattato di Medicina. 2017;19(1):1-7. doi: 10.1016/S1634-7358(16)81854-9.
16. McQuade RM, Bornstein JC, Nurgali K. Anti-colorectal cancer chemotherapy-induced diarrhoea: current treatments and side-effects. Int J Clin Med. 2014;05(7):393-406. doi: 10.4236/ijcm.2014.57054.
17. Ciardiello F, Tortora G. EGFR antagonists in cancer treatment. N Engl J Med. 2008 Mar 13;358(11):1160-74. doi: 10.1056/NEJMra0707704, PMID 18337605.
18. Folgueras AR, Pendas AM, Sanchez LM, Lopez Otin C. Matrix metalloproteinases in cancer: from new functions to improved inhibition strategies. Int J Dev Biol. 2004 Sep 1;48(5-6):411-24. doi: 10.1387/ijdb.041811af.
19. Metibemu DS, Oyeneyin OE, Omotoyinbo DE, Adeniran OY, Metibemu AO, Oyewale MB. Molecular docking and quantitative structure-activity relationship for the identification of novel phyto-inhibitors of matrix metalloproteinase-2. Sci Lett. 2020;8(2):61-8.
20. Roux PP, Topisirovic I. Signaling pathways involved in the regulation of mRNA translation. Mol Cell Biol. 2018 Jun 15;38(12):e00070-18. doi: 10.1128/MCB.00070-18, PMID 29610153.
21. Sithanandam G, Kolch W, Duh FM, Rapp UR. Complete coding sequence of a human B-raf cDNA and detection of B-raf protein kinase with isozyme-specific antibodies. Oncogene. 1990;5(12):1775-80. PMID 2284096.
22. Sithanandam G, Druck T, Cannizzaro LA, Leuzzi G, Huebner K, Rapp UR. B-raf and a B-raf pseudogene are located on 7q in man. Oncogene. 1992 Apr 1;7(4):795-9. PMID 1565476.
23. Li B, Liang J, Lu F, Zeng G, Zhang J, Ma Y. Discovery of novel inhibitor for Wnt/β-catenin pathway by tankyrase 1/2 structure-based virtual screening. Molecules. 2020 Apr 6;25(7):1680. doi: 10.3390/molecules25071680, PMID 32268564.
24. Liao HY, Da CM, Liao B, Zhang HH. Roles of matrix metalloproteinase-7 (MMP-7) in cancer. Clin Biochem. 2021 Jun 1;92:9-18. doi: 10.1016/j.clinbiochem.2021.03.003, PMID 33713636.
25. Ryu H, Nam KY, Kim HJ, Song JY, Hwang SG, Kim JS. Discovery of a novel triazolopyridine derivative as a tankyrase inhibitor. Int J Mol Sci. 2021 Jul 8;22(14):7330. doi: 10.3390/ijms22147330, PMID 34298950.
26. Wang YB, Shi Q, Li G, Zheng JH, Lin J, Qiu W. MicroRNA-488 inhibits progression of colorectal cancer via inhibition of the mitogen-activated protein kinase pathway by targeting claudin-2. Am J Physiol Cell Physiol. 2019 Jan 1;316(1):C33-47. doi: 10.1152/ajpcell.00047.2018, PMID 30207785.
27. Li R, Ma X, Song Y, Zhang Y, Xiong W, Li L. Anti-colorectal cancer targets of resveratrol and biological molecular mechanism: analyses of network pharmacology, human and experimental data. J Cell Biochem. 2019 Jul;120(7):11265-73. doi: 10.1002/jcb.28404, PMID 30719773.
28. Srivastava A, Rai S, Bisht D, Sachan M, Jit BP, Srivastava S. Targeting the altered tyrosine kinases in colorectal cancer: from inhibitors to drugs. Inprotein Kinase Inhibitors 2022 Jan 1;361-91.
29. Black LE, Longo JF, Carroll SL. Mechanisms of receptor tyrosine-protein kinase ErbB-3 (ERBB3) action in human neoplasia. Am J Pathol. 2019;189(10):1898-912. doi: 10.1016/j.ajpath.2019.06.008, PMID 31351986.
30. Black LE, Longo JF, Carroll SL. Mechanisms of receptor tyrosine-protein kinase ErbB-3 (ERBB3) action in human neoplasia. Am J Pathol. 2019 Oct 1;189(10):1898-912. doi: 10.1016/j.ajpath.2019.06.008, PMID 31351986.
31. Yu H, Yue X, Zhao Y, Li X, Wu L, Zhang C. LIF negatively regulates tumor-suppressor p53 through Stat3/ID1/MDM2 in colorectal cancers. Nat Commun. 2014 Oct 17;5(1):5218. doi: 10.1038/ncomms6218, PMID 25323535.
32. Hernandez Borrero LJ, El-Deiry WS. Tumor suppressor p53: biology, signaling pathways, and therapeutic targeting. Biochim Biophys Acta Rev Cancer. 2021 Aug 1;1876(1):188556. doi: 10.1016/j.bbcan.2021.188556, PMID 33932560.
33. Lazarev VF, Guzhova IV, Margulis BA. Glyceraldehyde-3-phosphate dehydrogenase is a multifaceted therapeutic target. Pharmaceutics. 2020 May 2;12(5):416. doi: 10.3390/pharmaceutics12050416, PMID 32370188.
34. Tang Z, Yuan S, Hu Y, Zhang H, Wu W, Zeng Z. Over-expression of GAPDH in human colorectal carcinoma as a preferred target of 3-bromopyruvate propyl ester. J Bioenerg Biomembr. 2012 Feb;44(1):117-25. doi: 10.1007/s10863-012-9420-9, PMID 22350014.
35. He JX, Yang CH, Miao ZH. Poly(ADP-ribose) polymerase inhibitors as promising cancer therapeutics. Acta Pharmacol Sin. 2010 Sep;31(9):1172-80. doi: 10.1038/aps.2010.103, PMID 20676117.
36. Gao Y, Zhou S, Xu Y, Sheng S, Qian SY, Huo X. Nitric oxide synthase inhibitors 1400W and L-NIO inhibit angiogenesis pathway of colorectal cancer. Nitric Oxide. 2019 Feb 1;83:33-9. doi: 10.1016/j.niox.2018.12.008, PMID 30590117.

37. Mashimo M, Shimizu A, Mori A, Hamaguchi A, Fukushima K, Seira N. PARP14 regulates EP4 receptor expression in human colon cancer HCA-7 cells. Biochem Biophys Res Commun. 2022 Oct 1;623:133-9. doi: 10.1016/j.bbrc.2022.07.055, PMID 35914351.
38. Castro ED, Mathias PPM, Batista WL, Sato AYS, Toledo MS, de Almeida VT. Knockdown of the inducible nitric oxide synthase (NOS2) splicing variant S3 promotes autophagic cell death from nitrosative stress in SW480 human colon cancer cells. Cell Biol Int. 2022 Jan;46(1):158-69. doi: 10.1002/cbin.11717, PMID 34719858.
39. Doman AJ, Tommasi S, Perkins MV, McKinnon RA, Mangoni AA, Nair PC. Chemical similarities and differences among inhibitors of nitric oxide synthase, arginase and dimethylarginine dimethylaminohydrolase-1: implications for the design of novel enzyme inhibitors modulating the nitric oxide pathway. Bioorg Med Chem. 2022;72:116970. doi: 10.1016/j.bmc.2022.116970, PMID 36063653.
40. Tse AN, Carvajal R, Schwartz GK. Targeting checkpoint kinase 1 in cancer therapeutics. Clin Cancer Res. 2007;13(7):1955-60. doi: 10.1158/1078-0432.CCR-06-2793, PMID 17404075.
41. Bucher N, Britten CD. G2 checkpoint abrogation and checkpoint kinase-1 targeting in the treatment of cancer. Br J Cancer. 2008;98(3):523-8. doi: 10.1038/sj.bjc.6604208, PMID 18231106.
42. Sun J, Li M, Lin T, Wang D, Chen J, Zhang Y. Cell cycle arrest is an important mechanism of action of compound Kushen injection in the prevention of colorectal cancer. Sci Rep. 2022;12(1):4384. doi: 10.1038/s41598-022-08336-4. PMID 35288618.
43. Fujita KI, Kubota Y, Ishida H, Sasaki Y. Irinotecan, a key chemotherapeutic drug for metastatic colorectal cancer. World J Gastroenterol. 2015;21(43):12234-48. doi: 10.3748/wjg.v21.i43.12234, PMID 26604633.
44. Falcone A, Ricci S, Brunetti I, Pfanner E, Allegrini G, Barbara C. Phase III trial of infusional fluorouracil, leucovorin, oxaliplatin, and irinotecan (FOLFOXIRI) compared with infusional fluorouracil, leucovorin, and irinotecan (FOLFIRI) as first-line treatment for metastatic colorectal cancer: the Gruppo Oncologico Nord Ovest. J Clin Oncol. 2007;25(13):1670-6. doi: 10.1200/JCO.2006.09.0928, PMID 17470860.
45. Si J, Zhao X, Gao S, Huang D, Sui M. Advances in delivery of irinotecan (CPT-11) active metabolite 7-ethyl-10-hydroxycamptothecin. Int J Pharm. 2019;568:118499. doi: 10.1016/j.ijpharm.2019.118499, PMID 31299338.
46. Stintzing S, Modest DP, Rossius L, Lerch MM, von Weikersthal LF, Decker T. FOLFIRI plus cetuximab versus FOLFIRI plus bevacizumab for metastatic colorectal cancer (FIRE-3): a post-hoc analysis of tumour dynamics in the final RAS wild-type subgroup of this randomised open-label phase 3 trial. Lancet Oncol. 2016;17(10):1426-34. doi: 10.1016/S1470-2045(16)30269-8, PMID 27575024.
47. Fan Y, Mansoor N, Ahmad T, Khan RA, Czejka M, Sharib S. Physiologically based pharmacokinetic modeling for predicting irinotecan exposure in human body. Oncotarget. 2017;8(29):48178-85. doi: 10.18632/oncotarget.18380, PMID 28636998.
48. Mullard A. Re-assessing the rule of 5, two decades on. Nat Rev Drug Discov. 2018;17(11):777. doi: 10.1038/nrd.2018.197, PMID 30374178.
49. Mahmoudi A, Jaafari MR, Ramezanian N, Gholami L, Malaekeh Nikouei B. BR2 and CyLoP1 enhance *in vivo* SN38 delivery using pegylated PAMAM dendrimers. Int J Pharm. 2019;564:77-89. doi: 10.1016/j.ijpharm.2019.04.037, PMID 30991135.
50. Tatusova T, DiCuccio M, Badretdin A, Chetvernin V, Nawrocki EP, Zaslavsky L, Ostell J. NCBI prokaryotic genome annotation pipeline. Nucleic Acids Research. 2016;44(14):6614-24. doi: 10.1093/nar/gkw569, PMID 27342282.
51. Kümper M, Hessenthaler S, Zamek J, Niland S, Pach E, Mauch C, Zigrino P. Loss of endothelial cell matrix metalloproteinase 14 reduces melanoma growth and metastasis by increasing tumor vessel stability. Journal of Investigative Dermatology. 2022;142(7):1923-33. doi: 10.1016/j.jid.2021.12.016, PMID 34968503.
52. Tanabe H, Suzuki T, Ohishi T, Isemura M, Nakamura Y, Unno K. Effects of epigallocatechin-3-gallate on matrix metalloproteinases in terms of its anticancer activity. Molecules. 2023;28(2):525. doi: 10.3390/molecules28020525, PMID 36677584.
53. Nelson AR, Fingleton B, Rothenberg ML, Matrisian LM. Matrix metalloproteinases: biologic activity and clinical implications. J Clin Oncol. 2000;18(5):1135. doi: 10.1200/JCO.2000.18.5.1135, PMID 10694567.
54. Huang H, Park S, Zhang H, Park S, Kwon W, Kim E. Targeting AKT with costunolide suppresses the growth of colorectal cancer cells and induces apoptosis *in vitro* and *in vivo*. J Exp Clin Cancer Res. 2021;40(1):114. doi: 10.1186/s13046-021-01895-w. PMID 33785035.
55. Saglam O, Garrett CR, Boulware D, Sayegh Z, Shibata D, Malafa M, Coppola D. Activation of the serine/threonine protein kinase AKT during the progression of colorectal neoplasia. Clinical Colorectal Cancer. 2007;6(9):652-6. doi: 10.3816/CCC.2007.n.034, PMID 17945038.
56. Kudryavtseva AV, Lipatova AV, Zaretsky AR, Moskalev AA, Fedorova MS, Rasskazova AS, Krasnov GS. Important molecular genetic markers of colorectal cancer. Oncotarget. 2016;7(33):53959-83. doi: 10.18632/oncotarget.9796, PMID 27276710.
57. Hussain MRM, Baig M, Mohamoud HSA, Ulhaq Z, Hoessli DC, Khogeer GS, Al-Aama JY. BRAF gene: from human cancers to developmental syndromes. Saudi Journal of Biological Sciences. 2015;22(4):359-73. doi: 10.1016/j.sjbs.2014.10.002, PMID 26150740.
58. Li B, Liang J, Lu F, Zeng G, Zhang J, Ma Y. Discovery of novel inhibitor for Wnt/β-catenin pathway by tankyrase 1/2 structure-based virtual screening. Molecules. 2020;25(7):1680. doi: 10.3390/molecules25071680, PMID 32268564.
59. Jang MK, Mashima T, Seimiya H. Tankyrase inhibitors target colorectal cancer stem cells via AXIN-dependent downregulation of c-KIT tyrosine Kinase Tankyrase. Mol Cancer Ther. 2020;19(3):765-76. doi: 10.1158/1535-7163.MCT-19-0668, PMID 31907221.
60. Shelley JC, Cholleti A, Frye LL, Greenwood JR, Timlin MR, Uchimaya M. Epik: a software program for pK(a) prediction and protonation state generation for drug-like molecules. J Comput Aided Mol Des. 2007;21(12):681-91. doi: 10.1007/s10822-007-9133-z, PMID 17899391.
61. Kumar TA, Ajay Kumar TV, Athavan AAS, Loganathan C, Saravanan K, Kabilan S, Parthasarathy V. Design, 3D QSAR modeling and docking of TGF-β type I inhibitors to target cancer. Comput Biol Chem. 2018;76:232-44. doi: 10.1016/j.compbiolchem.2018.07.011, PMID 30077902.
62. Balachandran P, V Ajay Kumar VA, T Parthasarathy V, Parthasarathy V. Screening of potential anticancer compounds from sargassum wightii to target breast cancer specific HER2 receptor using in-silico analysis. The Natural Products Journal. 2016;6(2):108-15. doi: 10.2174/2210315506666160218224112.
63. Kalirajan R, Sankar S, Jubie S, Gowramma B. Molecular docking studies and in-silico ADMET screening of some novel oxazine substituted 9-anilinoacridines as topoisomerase II inhibitors. Indian J Pharm Educ Res. 2017;51(1):110-5. doi: 10.5530/ijper.51.1.15.
64. Banks JL, Beard HS, Cao Y, Cho AE, Damm W, Farid R, Levy RM. Integrated modeling program, applied chemical theory (Impact). J Comput Chem. 2005;26(16):1752-80. doi: 10.1002/jcc.20292, PMID 16211539.
65. Muralikrishnan A, Kubavat J, Vasava M, Jupudi S, Biju N. Investigation of anti-sars cov-2 activity of some tetrahydro curcumin derivatives: an *in silico* study. Int J App Pharm. 2023;15(1):333-9. doi: 10.22159/ijap.2023v15i1.46288.
66. Martorana F, Motta G, Pavone G, Motta L, Stella S, Vitale SR, Vigneri P. AKT inhibitors: new weapons in the fight against breast cancer?. Frontiers in Pharmacology. 2021;12:662232. doi: 10.3389/fphar.2021.662232, PMID 33995085.
67. Friesner RA, Murphy RB, Repasky MP, Frye LL, Greenwood JR, Halgren TA, Mainz DT. Extra precision glide: docking and scoring incorporating a model of hydrophobic enclosure for protein-ligand

complexes. Journal of Medicinal Chemistry. 2006;49(21):6177-96. doi: 10.1021/jm051256o, PMID 17034125.

68. Lipinski CA. Lead-and drug-like compounds: the rule-of-five revolution. Drug Discov Today Technol. 2004 Dec;1(4):337-41. doi: 10.1016/j.ddtec.2004.11.007. PMID: 24981612.
69. Anonymous. Schrodinger release. New York: QikProp, Schrodinger, LLC; 2018.
70. Anonymous. Schrodinger release. Impact. Protein Preparation Wizard; 2018.
71. Kalirajan R, Sankar S, Jubie S, Gowramma B. Molecular docking studies and in-silico ADMET screening of some novel oxazine substituted 9-anilinoacridines as topoisomerase II inhibitors. Indian J Pharm Educ Res. 2017;51(1):110-5. doi: 10.5530/ijper.51.1.15.
72. Wary, Rakesh, Sivaraj, Sarany A, Gurukarthikeyana RKP, Mari S, Suraja GD, Kannayiram Gomathi. Chitosan gallic acid microsphere incorporated collagen matrix for chronic wounds: Biophysical and biochemical characterization. Int J Pharm Pharm Sci. 2014;6:94-100.
73. National Cancer Institute (NCI). Akt inhibitor MK2206. In: Treating patients with previously treated colon or rectal cancer that is metastatic or locally advanced and cannot be removed by surgery; 2019. Available from: https://beta.clinicaltrials.gov/study/NCT01802320.